

Flight-Test Data-Driven High-Angle-of-Attack Dynamics Modeling via LSTM-Polynomial Hybrid Approach

Zhang Zhengang[1,2], Zhao Huan[1,2], Zhang Weifeng[1,2], He Jiayi[1,2] & Gao Zhenghong[1,2]

[1]Northwestern Polytechnical University, Xi'an, Shaanxi, 710072, China
[2]National Key Laboratory of Aircraft Configuration Design, Xi'an 710072, China

Abstract

To address the significant accuracy degradation of traditional aerodynamic models in the stall/near-stall regions due to strong nonlinearities and unsteady effects, this paper proposes a hybrid modeling method combining a polynomial model and a Long Short-Term Memory (LSTM) network. Based on rigid-body dynamic equations, flight-test data were filtered, and aerodynamic coefficients were inversely identified to construct a high-quality dataset for modeling. The proposed framework employs a polynomial model with explicit physical meaning as the backbone to capture the main nonlinear and quasi-static trends of aerodynamic forces. Concurrently, an LSTM network is cascaded as a residual corrector to compensate for hysteresis effects and higher-order unsteady characteristics that are difficult for traditional models to characterize, by learning from historical state sequences. This architecture is designed to structurally balance the physical foundation of polynomial models with the high-accuracy advantage of data-driven models. Validation was performed by integrating the identified model into a six-degree-of-freedom (6-DoF) flight simulation environment. Results demonstrate that the hybrid model achieves weighted relative prediction errors of 0.35% for angle of attack, 0.47% for normal load factor, and 2.65% for pitch rate during stall maneuvers. This work provides an effective technical pathway for high-fidelity unsteady aerodynamic modeling, combining physical interpretability with data-driven precision.

Keywords: High-angle-of-attack characteristics; Aerodynamic modeling; Long Short-Term Memory (LSTM) network; Flight test; Grey-box model

1. Introduction

When an aircraft approaches or enters a stall condition, its aerodynamic forces and moments exhibit strong nonlinear, unsteady, and hysteretic behavior due to large-scale flow separation and the generation, development, and breakdown of vortices[1-2]. Specifically, the dynamic stall process involves the formation of a leading-edge vortex that travels downstream, causing a significant overshoot in lift followed by a sudden drop when the vortex sheds. This cyclic vortex evolution creates a pronounced lift-hysteresis loop with respect to the angle of attack, whose width can exceed 5°-10° depending on the pitching rate and airfoil geometry. Such hysteresis directly violates the fundamental assumption of static aerodynamic models, which assume instantaneous mapping between states and

https://doi.org/10.71945/icas2026_0269

coefficients. Accurately modeling such complex aerodynamic behavior is critical for the safe expansion of flight envelopes, the design and validation of advanced control laws, and the development of high-fidelity flight simulators.

Traditional aerodynamic modeling methods primarily rely on wind tunnel test data and parametric models[3-5]. Polynomial models are widely used due to their concise form and parameters with clear physical meanings[6]. By expressing aerodynamic coefficients as functions of state variables (such as angle of attack and angular rates) and their coupling terms, these models can effectively characterize nonlinear static and quasi-static behaviors within a certain range. However, in stall/near-stall regions, the flow exhibits significant memory effects and dynamic hysteresis. The aerodynamic coefficients depend not only on the current state but are also closely related to the historical path of state variations. Traditional polynomial models are essentially "memoryless" static mappings, making it difficult for them to accurately capture such complex unsteady dynamics. Consequently, their prediction accuracy and reliability face severe challenges in these regions.

In recent years, data-driven methods have provided new avenues for complex system modeling[7-9]. Deep learning techniques, particularly Recurrent Neural Networks (RNNs)[10] and their improved variant—Long Short-Term Memory (LSTM) networks—have achieved remarkable success in time series prediction and system identification, owing to their powerful capability to extract temporal features and learning long-range dependencies[11] . Existing studies have attempted to directly apply networks like LSTM for aerodynamic coefficient modeling, demonstrating a good ability to fit complex nonlinear dynamics. However, purely data-driven "black-box" models often lack physical interpretability: they may produce physically implausible predictions when extrapolating outside the training envelope, and their internal parameters have no direct correspondence to aerodynamic phenomena such as vortex shedding time scales. Their generalization performance heavily depends on the coverage of the training data, and their predictions under unseen or extreme conditions lack reliability. This limitation restricts their direct application in safety-critical aeronautical engineering fields.

To address the contradiction, this paper proposes a polynomial-LSTM hybrid modeling framework, aiming to construct a "grey-box" model that combines physical interpretability with high prediction accuracy. The core philosophy is to decompose the aerodynamic coefficient into a physically interpretable main term (polynomial) and a data-driven residual term (LSTM). This decomposition not only improves prediction accuracy but also maintains model transparency, because the polynomial part already captures the dominant physics while the LSTM only compensates for the remaining complex dynamics. The core idea is: utilizing the polynomial model to establish the fundamental physical framework for aerodynamic forces, capturing their main nonlinear static characteristics and low-order dynamic responses, thereby ensuring model transparency and a basis for extrapolation. Simultaneously, an LSTM network is introduced as a dedicated dynamic residual corrector. Taking historical state sequences from previous time steps as input, it is designed to specifically learn and compensate for the higher-order unsteady effects and complex hysteresis dynamics that the

polynomial model fails to represent. Unlike direct black-box LSTM modeling, this residual-learning architecture reduces the difficulty of network training because the target residual typically has a smaller magnitude and a near-zero mean, which alleviates the vanishing gradient problem and accelerates convergence. This structured fusion strategy aims to retain the robustness of parametric models while incorporating the fine-grained modeling capability of data-driven models for complex dynamics.

2. Polynomial-LSTM Hybrid Modeling Theoretical Framework

2.1 Overall Architecture Design

To overcome the insufficiency of traditional aerodynamic models in representing complex unsteady effects in stall/near-stall regions, this paper proposes a hybrid modeling framework that integrates parametric models with data-driven methods. The core concept is to use a polynomial model with explicit physical meaning as the backbone, capturing the static nonlinearities and primary dynamic trends of the aerodynamic forces, while simultaneously introducing a Long Short-Term Memory (LSTM) network as a dynamic residual corrector to learn and compensate for hysteresis and higher-order unsteady characteristics that the polynomial model fails to describe accurately.

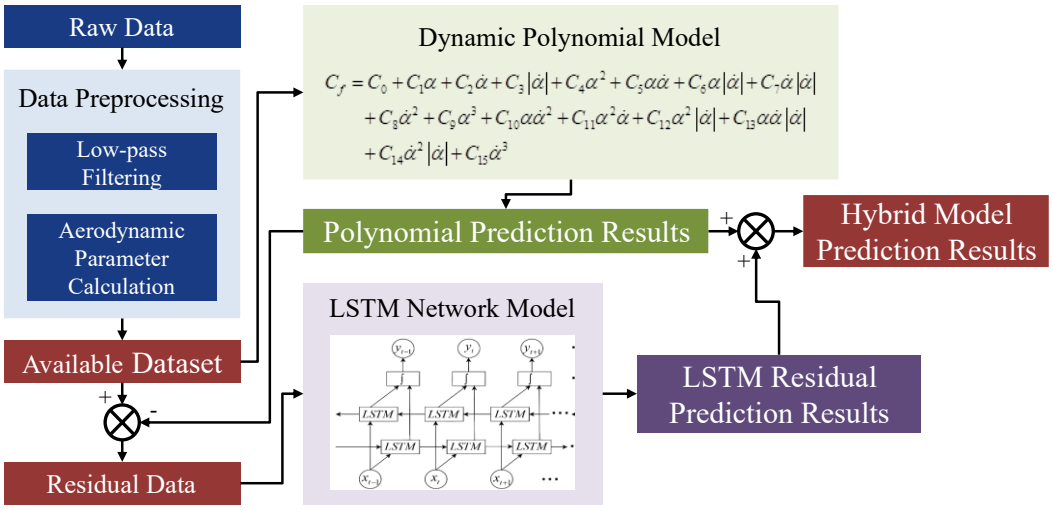


Figure 1 - Flowchart of the overall methodology architecture.

The overall architecture of this hybrid model is illustrated in Figure 1. For the target aerodynamic force or moment coefficient, its final predicted value is constituted by the linear superposition of two components:

$$C_f^{out} = C_{f0} + \Delta C_f^{LSTM} \tag{1}$$

where C_{f0} is the predicted output of the polynomial base model at time, characterizing the quasi-static and low-frequency dynamic response of the aerodynamic force to the current flight state. ΔC_f^{LSTM} is the output of the LSTM residual correction network. It is a function that depends on a sequence of recent historical flight states, used to capture the aerodynamic fluctuations caused by flow memory effects (such as vortex shedding, hysteresis in separated flow reattachment) that cannot be sufficiently described by instantaneous state variables. In essence, this "base + residual" grey-box

design balances two competing goals: it retains the physical interpretability and extrapolation robustness of parametric models, while harnessing the LSTM's strength in learning complex temporal patterns from data.

2.2 Polynomial model

To address the nonlinear and unsteady characteristics between aerodynamic force/moment and flight state parameters in modern aircraft flight, a polynomial algebraic model is employed for aerodynamic force/moment identification. This model can, to a certain extent, characterize the nonlinear effects of aerodynamic forces and changes in dynamic aerodynamic characteristics induced by unsteady flow separation.

Taking pitch oscillation as an example, the primary longitudinal aerodynamic forces and moments are expressed as polynomial functions of the angle of attack α and the angle of attack rate $\dot{\alpha}$:

$$C_f = C_0 + C_1\alpha + C_2\alpha^2 + C_3\dot{\alpha} + C_4|\dot{\alpha}| + C_5\alpha\dot{\alpha} + C_6\alpha|\dot{\alpha}| + C_7\dot{\alpha}|\dot{\alpha}| + C_8\dot{\alpha}^2 \tag{2}$$

Here, C_f represents aerodynamic force and moment coefficients, such as the lift coefficient C_L, drag coefficient C_D, pitch moment coefficient C_m, etc.

Given the strong nonlinearity and dynamic coupling characteristics of aerodynamic forces at high angles of attack, and based on the proposed theoretical framework, a high-order polynomial form incorporating the angle of attack α, pitch rate q, and their coupling terms is selected for modeling. Using a longitudinal aerodynamic coefficient as an example, its identification model can be specifically formulated as:

$$C_f = C_0 + C_1\alpha + C_2\dot{\alpha} + C_3de + C_4q + C_5\alpha^2 + C_6\dot{\alpha}^2 + C_7de^2 + C_8q^2 + ... \tag{3}$$

To adequately capture the nonlinear characteristics of the aerodynamic force, second-order terms and cross-coupling terms are introduced into the basic polynomial model:

Second-order terms: α^2, $\dot{\alpha}^2$, de^2, q^2

Cross-coupling terms: $\alpha\dot{\alpha}$, αde, αq, $\dot{\alpha} de$, $\dot{\alpha} q$, deq

Although the polynomial model incorporates instantaneous dynamic terms, its output at any given time depends only on the current values of these variables. In other words, the model does not possess an internal state that accumulates or retains information from previous time steps. Consequently, it is incapable of reproducing the pronounced hysteresis loops and path-dependent behavior observed in stall maneuvers, where the aerodynamic response is influenced by the entire history of motion, not just the instantaneous condition. This inherent limitation motivates the introduction of a complementary LSTM module that can explicitly model temporal dependencies and capture long-term memory effects. Thus, the polynomial model serves as a physically grounded baseline, but it leaves systematic residuals that the LSTM is designed to correct.

2.3 LSTM Residual Model

While the polynomial model can characterize certain instantaneous unsteady responses by incorporating dynamic terms such as the rate of change of angle of attack, its ability to represent

history-dependent phenomena is fundamentally limited because it lacks a state memory mechanism. The model's output at each time step is a function solely of the current state vector (including its time derivatives), without any knowledge of how that state was reached. As a result, it struggles to capture the strong hysteresis effects and complex path dependence exhibited at high angles of attack due to processes like flow separation and vortex evolution. To further enhance the model's ability to represent higher-order nonlinearities, unsteady dynamics, and coupling effects between multiple degrees of freedom, this paper introduces a Long Short-Term Memory (LSTM) network as a dynamic residual corrector.

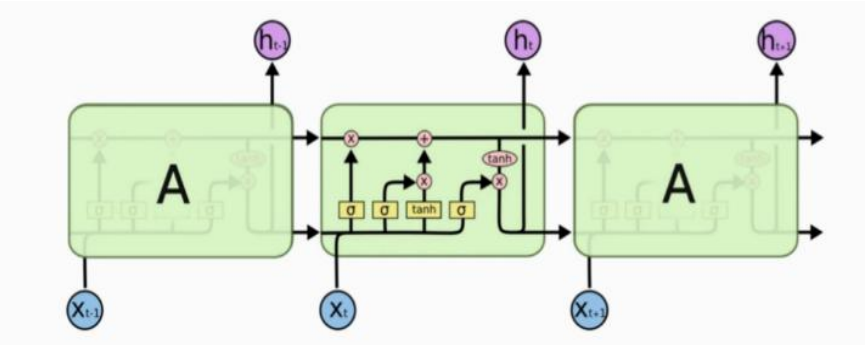


Figure 2 - Architecture of the LSTM neural network.

LSTM is a specialized recurrent neural network architecture designed to overcome the vanishing/exploding gradient problem of traditional RNNs, enabling it to learn long-term dependencies. The core of LSTM is the cell state c_t, which acts as a memory conveyor belt, and three gating mechanisms that control the flow of information: the forget gate f_t, the input gate i_t, and the output gate o_t. At each time step t, given the current input x_t (flight state features), the previous hidden state h_{t-1}, and the previous cell state c_{t-1}, the LSTM updates as follows(as illustrated in Figure 2):

$$\begin{aligned} f_t &= \sigma\left(W_f\left[h_{t-1}, x_t\right] + b_f\right) \\ i_t &= \sigma\left(W_i\left[h_{t-1}, x_t\right] + b_i\right) \\ \tilde{c}_t &= \tanh\left(W_c\left[h_{t-1}, x_t\right] + b_c\right) \\ c_t &= f_t \odot c_{t-1} + i_t \odot \tilde{c}_t \\ o_t &= \sigma\left(W_o\left[h_{t-1}, x_t\right] b_o\right) \\ h_t &= o_t \odot \tanh\left(c_t\right) \end{aligned} \tag{4}$$

Where σ is the sigmoid activation function, $\odot$ denotes element-wise multiplication, W and b are learnable weights and biases. The forget gate determines how much of the past cell state to retain, the input gate controls how much new information to write, and the output gate filters the cell state to produce the hidden state. Through this gated architecture, LSTM can selectively remember or forget information over hundreds of time steps, making it ideal for modeling flow memory effects. LSTM, through the gating mechanisms of the input gate, forget gate, and output gate, can effectively learn long-term temporal dependencies.

Within this framework, the task of the LSTM network is to predict the residual between the polynomial model's output and the true aerodynamic data based on a time-series sequence containing current and historical flight states (such as angle of attack, angular rates, control surface deflections, etc.). This residual encompasses not only random errors but, more importantly, reflects three types of physical effects that the polynomial model fails to adequately describe due to structural and parametric limitations:

a. **Higher-order nonlinearity and unsteady hysteresis:** Complex dynamics such as strong nonlinearities and large hysteresis loops associated with deep stall and dynamic separation, whose time scales and dependencies fall beyond the representational scope of the polynomial model.
b. **Multi-degree-of-freedom coupling effects:** Dynamic couplings between lateral-directional and longitudinal motions (e.g., roll-yaw-pitch coupling) are difficult to fully characterize within a single longitudinal polynomial model.

Leveraging its gating mechanisms, the LSTM network can adaptively learn the implicit mapping relationships between these complex dynamics and historical states, thereby achieving accurate prediction of the residual. Importantly, instead of re-modeling the entire aerodynamic behavior from scratch, this network serves as an intelligent compensation term that dynamically corrects the structural residual inherent to the polynomial model.

In summary, the introduction of the LSTM residual corrector transforms the originally static polynomial model into a dynamic grey-box system. The polynomial part handles the instantaneous, quasi-static response, while the LSTM part accounts for the history-dependent, unsteady effects. This division of labor allows each component to focus on what it does best, leading to a model that is both physically interpretable and capable of high-accuracy prediction in stall/near-stall conditions.

3. Flight Test Data Description and Processing

3.1 Data Description

The data used in this paper are all sourced from high-angle-of-attack flight tests of a certain type of passenger aircraft.

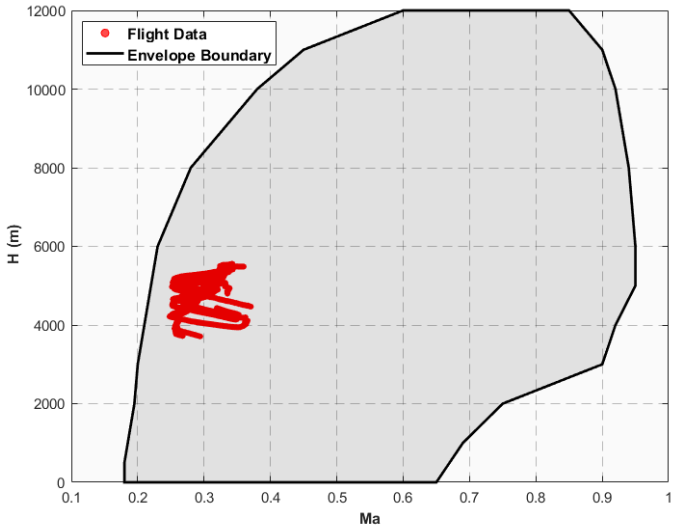


Figure 3 - Envelope distribution of the data points.

Figure 3 shows the distribution of data points within the flight envelope. As can be seen, the data points are primarily concentrated on the left boundary of the envelope, which is precisely the region where high-angle-of-attack events frequently occur. A total of 15 data sets were selected, all intentionally drawn from this high-angle-of-attack region on the left boundary to ensure that the modeling effort focuses on the most challenging flight regime.

To capture the dynamic aerodynamic characteristics in the stall/near-stall region, a longitudinal pulse-type control input was employed during the flight tests. The design of this input is critical for exciting unsteady aerodynamic effects while maintaining flight safety. Specifically, the pilot first slowly pulled the control column to steadily increase the aircraft's angle of attack to a target value. After a brief hold, the control column was then centered at a relatively faster speed, returning the control input to the trim position. This pattern of slow-increase and fast-return ensures that the aircraft experiences a gradual entry into the high-angle-of-attack region followed by a more rapid recovery, thereby generating a distinct hysteresis cycle that can be used for dynamic stall analysis. This input signal effectively excites dynamic modes of the aircraft, such as the short-period pitching mode, while ensuring flight safety. In summary, the selected data and the dedicated excitation maneuver provide a suitable foundation for identifying and validating the proposed hybrid model in the stall regime.

3.2 Data Preprocessing

Raw flight test data inevitably contain sensor noise and high-frequency interference, which would severely impact the accuracy and reliability if used directly for model identification. Therefore, the raw data underwent filtering preprocessing, and aerodynamic coefficients were inversely identified based on the dynamic equations to construct a high-quality modeling dataset.

In this study, a fourth-order Butterworth low-pass filter was applied to all time-series state data. This filter order was chosen to provide a good balance between sharp roll-off and minimal pass-band ripple. The filter was designed for zero-phase filtering to eliminate high-frequency noise without introducing phase lag, which is essential for preserving the temporal alignment between state

variables and aerodynamic responses. The filter's cutoff frequency was set to 4 Hz, a value selected based on the dominant frequency content of the aircraft's short-period mode (typically below 2 Hz), ensuring that the relevant dynamics are retained while higher-frequency noise is effectively suppressed. The effect of the filtered data is shown in Figure 4.

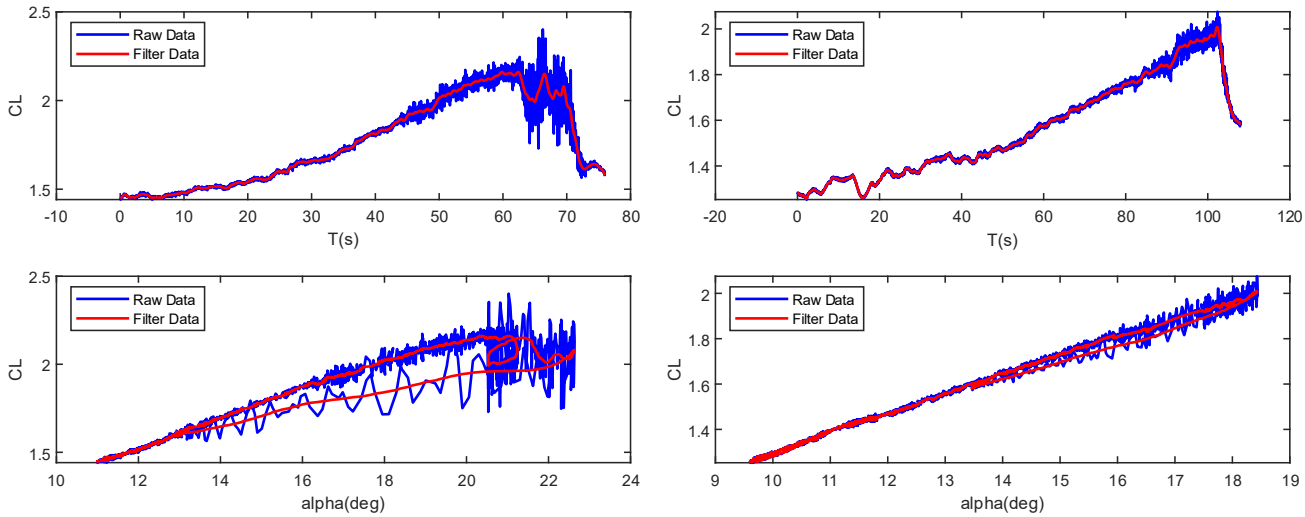


Figure 4 - Data filtering effect.

Based on the cleaned state variables, aerodynamic force and moment coefficients were inversely calculated according to the aircraft's rigid-body dynamic equations. This inverse identification step converts the filtered measurements into physically consistent aerodynamic coefficients, which serve as the ground truth for model training. The formulas for calculating the aerodynamic force coefficients and moment coefficients are as follows:

$$\begin{bmatrix} C_X \\ C_Y \\ C_Z \end{bmatrix} = \frac{m}{\bar{q}S}\left(\begin{bmatrix} a_x \\ a_y \\ a_z \end{bmatrix} - R_{bg}\begin{bmatrix} 0 \\ 0 \\ g \end{bmatrix}\right) \tag{5}$$

$$\begin{bmatrix} C_l \\ C_m \\ C_n \end{bmatrix} = I^{-1}\left(\begin{bmatrix} L \\ M \\ N \end{bmatrix}\right) \Big/ \left(\bar{q}S\left[b, \bar{c}, b\right]\right) \tag{6}$$

where m is the aircraft mass, $\bar{q} = 0.5\rho V^2$ is the dynamic pressure, S is the reference area, b and $\bar{c}$ are the wingspan and mean aerodynamic chord, respectively. $[a_x, a_y, a_z]^T$ are the body-axis linear accelerations, and R_{bg} is the transformation matrix from the Earth frame to the body frame, used to subtract the gravity component. The aerodynamic moments $[L, M, N]^T$ are solved from the Euler dynamic equations using angular accelerations and the inertia tensor I .

Through the above processing, time-synchronized flight state sequences with controlled noise and their corresponding physically consistent aerodynamic coefficient sequences were ultimately obtained. In summary, the preprocessing pipeline effectively transforms raw, noisy flight data into a clean, reliable dataset that captures the essential nonlinear and unsteady aerodynamic characteristics, thereby establishing a solid foundation for the subsequent hybrid model identification.

4. Modeling of Unsteady Aerodynamic Forces

4.1 Polynomial Model Parameter Identification

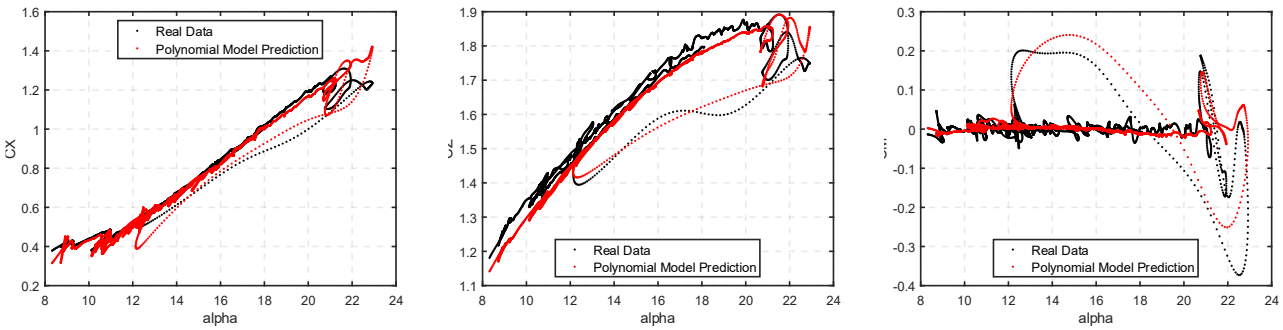
Parameters were identified using the least squares method. The least squares method is simple, easy to understand, and convenient to apply. The objective function is:

$$J(\theta)=\sum_{i=1}^{N}\left[y_i-\phi_i^T\theta\right]^2=\left\|Y-\Phi\theta\right\|^2 \tag{7}$$

Where Y is the observation data vector; Φ is the regression matrix; ϕ_i is the feature vector of the *i*-th sample.

To circumvent potential ill-conditioning issues with the normal equations and improve the stability of the numerical solution, a numerical method based on QR decomposition was used in this study to solve the aforementioned least squares problem. This approach avoids explicitly forming the normal equations, which can be nearly singular when the features are highly correlated, and provides better numerical accuracy.

Figure 5 shows the prediction performance of the polynomial model on the flight test data. Overall, the model performs well in predicting aerodynamic forces, but observable deviations remain in key parameters. For lift coefficient prediction, the model aligns well with the actual flight data, accurately reflecting the aircraft's basic lift characteristics. The prediction of the pitching moment coefficient shows more pronounced discrepancies, indicating limitations in the polynomial model's ability to capture nonlinear lift variations prior to stall. These discrepancies are most evident near the stall boundary, where the flow becomes unsteady and the hysteresis effect becomes significant.



(a)CX (b)CZ (c)CM

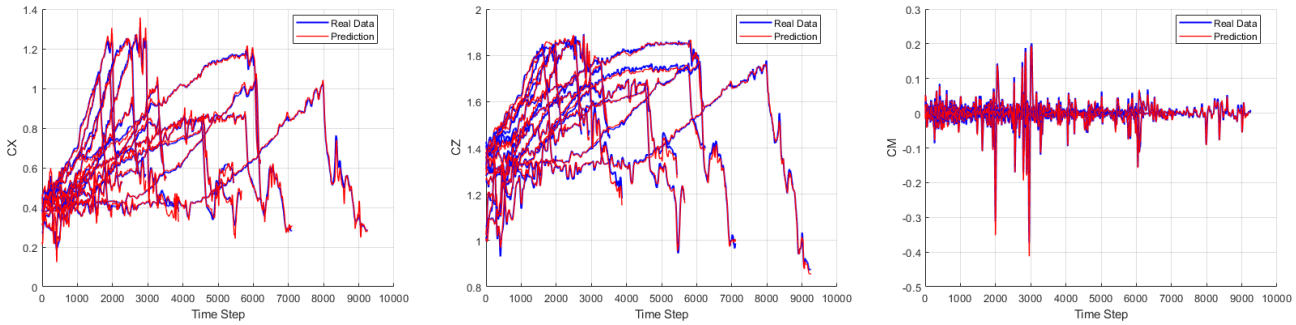
Figure 5 - Performance of the polynomial model on aerodynamic flight test data.

4.2 LSTM Residual Network Design and Training

To effectively capture temporal dependencies within the aerodynamic residual, a stacked network containing two LSTM layers was constructed. The network input is a historical state sequence with a length of 10 time steps, and input features include the angle of attack, pitch rate, sideslip angle, roll and yaw rates, and corresponding control surface deflections, among others. The sequence length of 10 was chosen based on the sampling rate and the expected duration of the flow memory effect (approximately 0.1 seconds), which is sufficient to cover the dominant unsteady dynamics. The first LSTM layer contains 64 hidden units, responsible for preliminary extraction of temporal features; the second LSTM layer contains 32 hidden units, used for further integration of higher-level dynamic

patterns. A Dropout layer with a rate of 0.2 follows each LSTM layer to enhance the model's generalization capability. The network finally outputs a scalar residual through a fully connected layer. The training target for the LSTM network is the residual between the polynomial model's predicted values and the true aerodynamic coefficients. Before training, the data underwent standardization. The network uses the mean squared error as the loss function, the Adam optimizer for parameter updates, with an initial learning rate set to 0.001 and a learning rate decay strategy employed. The training process incorporated an early stopping mechanism, halting training when the validation loss failed to decrease for 10 consecutive epochs to prevent overfitting.

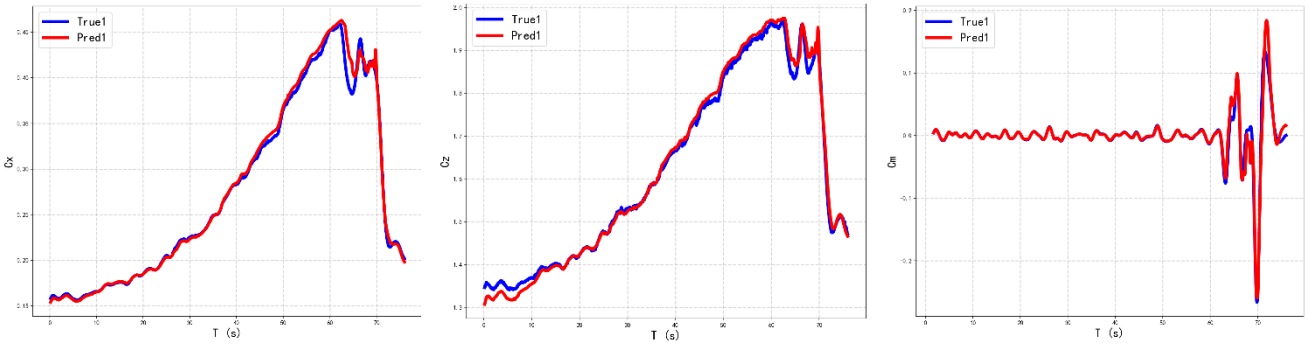
Figure 6 illustrates the residual prediction performance of the model on the training dataset. As shown, the LSTM network can effectively learn the residual patterns within the training data, with the predicted curve closely matching the true residual curve, indicating the network's capability to capture complex nonlinear temporal dependencies.



(a)CX (b)CZ (c)CM

Figure 6 - Model performance on training data.

Figure 7 demonstrates the model's prediction performance on an independent test dataset. Although not involved in training, the LSTM network can still accurately predict the residual trends on the test set, with its predicted curve maintaining consistency in amplitude and phase with the true residual. This indicates that the designed network structure possesses good generalization ability and can effectively estimate aerodynamic residuals under flight states not previously encountered.



(a)CX (b)CZ (c)CM

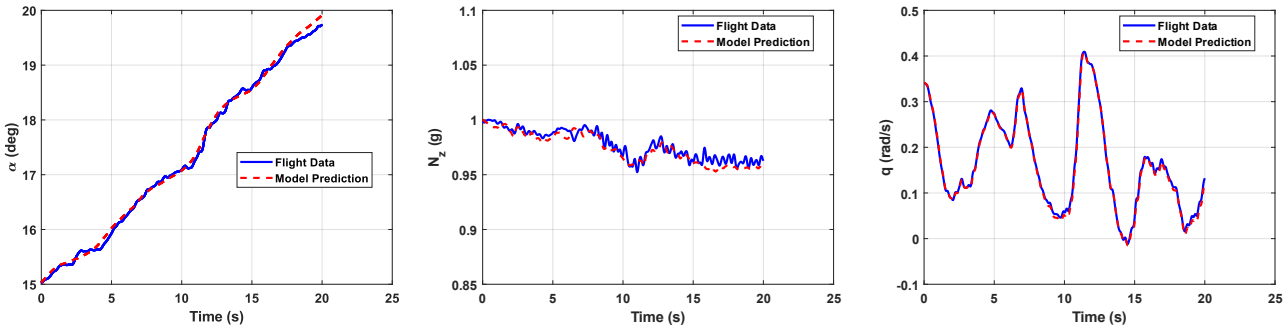
Figure 7 - Model performance on test data.

Taken together, Figures 6 and 7 show that it can be concluded that the constructed LSTM residual corrector can stably and reliably learn and predict the output residual of the polynomial model, laying the foundation for building a high-precision hybrid model.

4.3 Model Validation and Analysis

To evaluate the generalization capability and prediction accuracy of the proposed polynomial-LSTM hybrid model in a realistic dynamic environment, this section constructs an open-loop simulation verification environment based on the six-degree-of-freedom flight dynamics equations using Simulink. The model performance is then tested using a set of flight test data independent of the training set. In this open-loop setup, the hybrid model provides the aerodynamic coefficients at each time step, while the aircraft states are integrated from the equations of motion using the same measured control inputs as in the flight test. This configuration allows a direct comparison between the simulated state trajectories and the actual flight data.

Figure 8 presents the comparison results of this open-loop simulation verification. The results show good agreement between the model predictions and the flight-test data, particularly for the key parameters: angle of attack, normal load factor, and pitch rate.



(a)alpha (b)Nz (c)q

Figure 8 - Simulation verification results.

Table 1 Weighted Average Percentage Errors (WAPE) for Key State Parameters

State Parameter	Weighted Average Percentage Error	Engineering Criterion
Angle of Attack	0.35%	≤5%
Normal Load Factor	0.47%	≤5%
Pitch Rate	2.65%	≤5%

As shown in the table, the weighted relative errors are all at a relatively low level. This result confirms the effectiveness of the proposed hybrid modeling framework: by learning historical state sequences, the LSTM network successfully compensates for the inherent deficiencies of the polynomial model in characterizing higher-order unsteady and hysteresis characteristics, thereby significantly improving the overall prediction accuracy of the aerodynamic model in the stall region without sacrificing physical interpretability.

5. Conclusion

In response to the insufficient prediction accuracy of traditional aerodynamic models for complex nonlinear and unsteady characteristics in aircraft stall/near-stall regions, this paper proposes and validates a polynomial-LSTM hybrid modeling framework that integrates the advantages of physical models and data-driven methods. The framework operates as follows: it uses a polynomial model with explicit physical meaning as the foundation to capture the dominant nonlinear and quasi-static

trends of aerodynamic forces, thereby ensuring core interpretability. Simultaneously, it cascades a Long Short-Term Memory (LSTM) network as a dynamic residual corrector, specifically designed to learn and compensate for higher-order unsteady dynamics—caused by flow hysteresis, vortex dynamic evolution, and multi-degree-of-freedom coupling—that are difficult to parameterize with polynomials. This combination forms a complementary “grey-box” modeling strategy that balances physical transparency with data-driven precision.

Based on flight test data, this study constructed a high-quality dataset through systematic signal filtering and aerodynamic coefficient inversion, and completed the full engineering implementation from model identification and training to integrated verification. Open-loop simulation verification results show that, compared to the pure polynomial model, the proposed hybrid model achieves significant improvements in the prediction accuracy of key state parameters (angle of attack, normal load factor, pitch rate) during stall maneuvers. The weighted average relative errors are reduced to 0.35%, 0.47%, and 2.65%, respectively, all of which are well below the 5% engineering criterion. These results fully demonstrate the effectiveness of the proposed framework in enhancing the accuracy of stall-region dynamics modeling.

Overall, this work indicates that the hybrid architecture combining polynomials and LSTM provides an effective technical pathway for achieving high-precision, high-confidence unsteady aerodynamic force modeling. It holds clear engineering application value in fields such as flight simulation, control law design, and safety envelope expansion. Future work will focus on three directions: investigating the generalization capability of this framework across a wider flight envelope, further embedding physical constraints into the learning process, and exploring lightweight deployment of the model for real time applications.

6. Contact Author Email Address

Huan Zhao: huanzhao@nwpu.edu.cn

7. Copyright Statement

The authors confirm that they, and/or their company or organization, hold copyright on all of the original material included in this paper. The authors also confirm that they have obtained permission, from the copyright holder of any third party material included in this paper, to publish it as part of their paper. The authors confirm that they give permission, or have obtained permission from the copyright holder of this paper, for the publication and distribution of this paper as part of the ICAS proceedings or as individual off-prints from the proceedings.

8. Acknowledgement

This work was sponsored by the National Natural Science Foundation of China (NSFC) under grant No. 52572420 and the foundation of National Key Laboratory of Aircraft Configuration Design under grant No. JBGS-202502. These supports are gratefully acknowledged.

References

[1] Neves AF, Lawson NJ, Bennett CJ, Khanal B, and Hoff RI. Unsteady aerodynamics analysis and modelling of a slingsby firefly aircraft: detached-eddy simulation model and flight test validation. *Aerospace Science and Technology*, Vol. 106, 2020.

[2] Xu ZJ, Cao NY, Li CY, Luo YJ, Su E, Wang WZ, Tang W, Yao ZH, and Wang ZL. Digital mapping of surface turbulence status and aerodynamic stall on wings of a flying aircraft. *Nature Communications*, Vol. 14, No. 1, p. 2792, 2023.

[3] Goman MG, and Khrabrov AN. State-Space Representation of Aerodynamic Characteristics of an Aircraft at High Angles of Attack. *Journal of Aircraft*, Vol. 31, pp. 1109-1115, 1994.

[4] Lin GF, Lan C, and Brandon J. A generalized dynamic aerodynamic coefficient model for flight dynamics applications. *22nd Atmospheric Flight Mechanics Conference*, 1997.

[5] Abramov N, Khrabrov A, Kolinko K, and Goman M. Simple wings unsteady aerodynamics at high angles of attack - Experimental and modeling results. *24th Atmospheric Flight Mechanics Conference*, 1999.

[6] Wang LX, Zhao R, Xu K, Zhang Y, and Yue T. Identification and modeling method of longitudinal stall aerodynamic parameters of civil aircraft based on improved kirchhoff stall aerodynamic model. *Aerospace*, Vol. 10, No. 4, p. 333, 2023.

[7] Winter M, and Breitsamter C. Nonlinear identification via connected neural networks for unsteady aerodynamic analysis. *Aerospace Science and Technology*, Vol. 77, pp. 802-818, 2018.

[8] Chen SL, Gao ZH, Zhu XQ, Du YM, and Pang C. Unstable unsteady aerodynamic modeling based on least squares support vector machines with general excitation. Chinese Journal of Aeronautics Vol. 33, No. 10, pp. 2499-2509, 2020.

[9] Kumar A, and Ghosh AK. Decision Tree– and Random Forest–Based Novel Unsteady Aerodynamics Modeling Using Flight Data. *Journal of Aircraft*, Vol. 56, No. 1, pp. 403-409, 2019.

[10] Chen X, Zhan JX., Chen K, Wei ZC, and Cao Y. Unsteady aerodynamic modeling research and virtual flight test verification. *Journal of Experiments in Fluid Mechanics*, Vol. 36, No. 3, pp. 65-72, 2022.

[11] Li K, Kou JQ, and Zhang WW. Deep neural network for unsteady aerodynamic and aeroelastic modeling across multiple Mach numbers. *Nonlinear Dynamics*, Vol. 96, No. 3, pp. 2157-2177, 2019.